SEDIMENTOLOGY the journal of the International Association of Sedimentologists

Sedimentology (2013) doi: 10.1111/sed.12056

An empirical model of subcritical bedform migration

CHAN-YI MARTIN LIN and JEREMY G. VENDITTI
Department of Geography, Simon Fraser University, Burnaby, British Columbia, V5A 1S6, Canada (E-mail: jeremy_venditti@sfu.ca)

ABSTRACT

The ability to predict bedform migration in rivers is critical for estimating bed material load, yet there is no relation for predicting bedform migration (downstream translation) that covers the full range of conditions under which subcritical bedforms develop. Here, the relation between bedform migration rates and transport stage is explored using a field and several flume data sets. Transport stage is defined as the non-dimensional Shields stress divided by its value at the threshold for sediment entrainment. Statistically significant positive correlations between both ripple and dune migration rates and transport stage are found. Stratification of the data by the flow depth to grain-size ratio improved the amount of variability in migration rates that was explained by transport stage to *ca* 70%. As transport stage increases for a given depth to grain-size ratio, migration rates increase. For a given transport stage, the migration rate increases as the flow depth to grain-size ratio gets smaller. In coarser sediment, bedforms move faster than in finer sediment at the same transport stage. Normalization of dune migration rates by the settling velocity of bed sediment partially collapses the data. Given the large amount of variability that arises from combining data sets from different sources, using different equipment, the partial collapse is remarkable and warrants further testing in the laboratory and field.

Keywords Bedform migration, bedforms, dunes, ripples, sand-bedded rivers, sediment flux.

INTRODUCTION

The ability to predict bedform migration rates in rivers is critical for estimating bed-material load (Simons *et al.*, 1965; Church, 2006; Nittrouer *et al.*, 2008; McElroy & Mohrig, 2009). Migration refers to the downstream translation of a bedform as opposed to bedform deformation, which is change in the bedform shape (McElroy & Mohrig, 2009). Downstream translation is usually thought of as contributing to the bedload transport in the channel. McElroy & Mohrig (2009) argued that deformation contributes to the suspended load because, by definition, deformation occurs by removing sediment from the bedform.

It is difficult to estimate translation because empirical relations between migration rates and various flow parameters (for example, mean velocity, Froude number and velocity head) are not well-defined (Simons *et al.*, 1965). Models of bedform migration require a great deal of input information to produce predictions (e.g. Mohrig & Smith, 1996) and theoretical linear perturbation models that give the velocity of the fastest growing waveform are of little practical use. Methods for estimating sediment transport associated with bedform migration using time-lapsed observations of bed topography are improving (Van den Berg, 1987; Ten Brinke *et al.*, 1999; Villard & Church, 2003; McElroy & Mohrig, 2009), but require observational data which are often difficult and labour intensive to acquire and analyse.

Two physically based models of bedform migration have been proposed. Mohrig & Smith (1996) developed a model to calculate bedform migration rates where there was both bedload

and suspended load, by estimating the fraction of sediment moving over the crests of bedforms that bypasses the lee face. Particles with excursion lengths greater than the length of the bedform lee face were assumed not to contribute to bedform migration. These authors found that if all sediment that bypassed the dune crest was deposited on the lee face, the model overestimated dune migration rates. If no suspended sediment was deposited in the lee of the crests, the model under-estimated dune migration rates. Ultimately, bedform migration was found to be achieved by a constant exchange between the bedform and the water column. While these insights are useful, the model itself requires an inordinate amount of input data, including fractional sediment transport rates, making it inappropriate for sediment flux predictions.

Bartholdy *et al.* (2010) introduced a model for sediment flux associated with bedform migration that is based on sediment mechanics over dunes. While the model is useful, it is strictly applicable to bedload-dominated channels because the migration is calculated from the bedload transported over the dune crest, quantified using the bedload transport velocity. This approach ignores the significant amount of suspended material that can contribute to bed-material transport in mixed load and suspended load-dominated channels (Kostaschuk *et al.*, 2009; McElroy & Mohrig, 2009). Kostaschuk *et al.* (2009), for example, shows that *ca* 17% of the suspended bed-material load transported over the dune crest in the Río Paraná is deposited in the lee before it reaches the trough. There remains a need for a model that covers the entire range of transport conditions (bedload-dominated to suspended load-dominated) over which bedforms develop.

In light of this, empirical relations between fluid forcing and bedform migration could be quite useful. Here, the relation between transport stage and bedform migration rates is explored. Following Church (2006), the transport stage is defined as the ratio of the Shields number to the critical Shields number for sediment entrainment (τ_*/τ_{*c}). The Shields number is defined as:

$$\tau_* = \frac{\tau}{(\rho_s - \rho_w)gD} \quad (1)$$

where τ is the shear stress at the bed, ρ_s and ρ_w are the sediment and water densities, respectively, g is gravitational acceleration and D is the grain size of the sediment, which is usually taken to be D_{50}, the median grain size of the bed sediment (Raudkivi, 1967). The critical value of τ_* for sediment entrainment (τ_{*c}) varies with grain size (cf. Miller *et al.*, 1977; Yalin & Karahan, 1979b). Church (2006), building on earlier work by Dade & Friend (1998), used the transport stage to define the dominant modes of sediment motion in river channels. Bedload-dominated channels have $\tau_*/\tau_{*c} < 3{\cdot}3$, mixed bedload and suspended load channels have $3{\cdot}3 < \tau_*/\tau_{*c} < 33$ and suspended load-dominated channels have $\tau_*/\tau_{*c} > 33$. It is important to note that two channels can have the same transport stage, but different τ_* because of variability in τ_{*c}.

There is good reason to suspect that a fundamental relation exists between transport stage and migration rate. Transport stage is known to influence bedform geometry, which is known to influence migration rates. Yalin (Yalin, 1972; Yalin & Karahan, 1979a) and later van Rijn (1984) demonstrated that the aspect ratio of bedforms, defined as the height (H) to length (L) ratio, depends on the transport stage. Figure 1 summarizes observations of ripple and dune H/L for equilibrium conditions, where the bedforms are fully adjusted to the imposed flow. Bedform aspect ratio is small when τ_* is just above τ_{*c}, it increases with τ_*/τ_{*c}, then decreases at higher transport stages. Ripples and dunes show the same trend, but ripples reach a maximum H/L at a lower transport stage than dunes and the maximum aspect ratio is higher for ripples than for dunes. Lin (2011) showed that this pattern occurs because equilibrium bedform heights are smaller under bedload-dominated conditions and increase with transport stage, reaching a maximum at a mixed transport stage. Heights decline with increasing transport stage under suspended load-dominated conditions until they wash out to a plane bed. Equilibrium lengths increase with transport stage, giving rise to the parabola shape of the relation between H/L and transport stage.

In addition to the relation between transport stage and bedform dimensions, there are well-defined relations between bedform geometry (H, L and H/L) and migration rates (Allen, 1973; Coleman & Melville, 1994; Venditti *et al.*, 2005) (Fig. 1). The length and height of individual dunes in a bed configuration vary in space and time as they migrate under steady and uniform flow (Allen, 1973; Leclair, 2002; Bridge, 2003; Venditti *et al.*, 2005; McElroy & Mohrig, 2009). If the sediment transport rate is constant, the speed of an individual bedform is controlled by its size. The migration rate of an individual

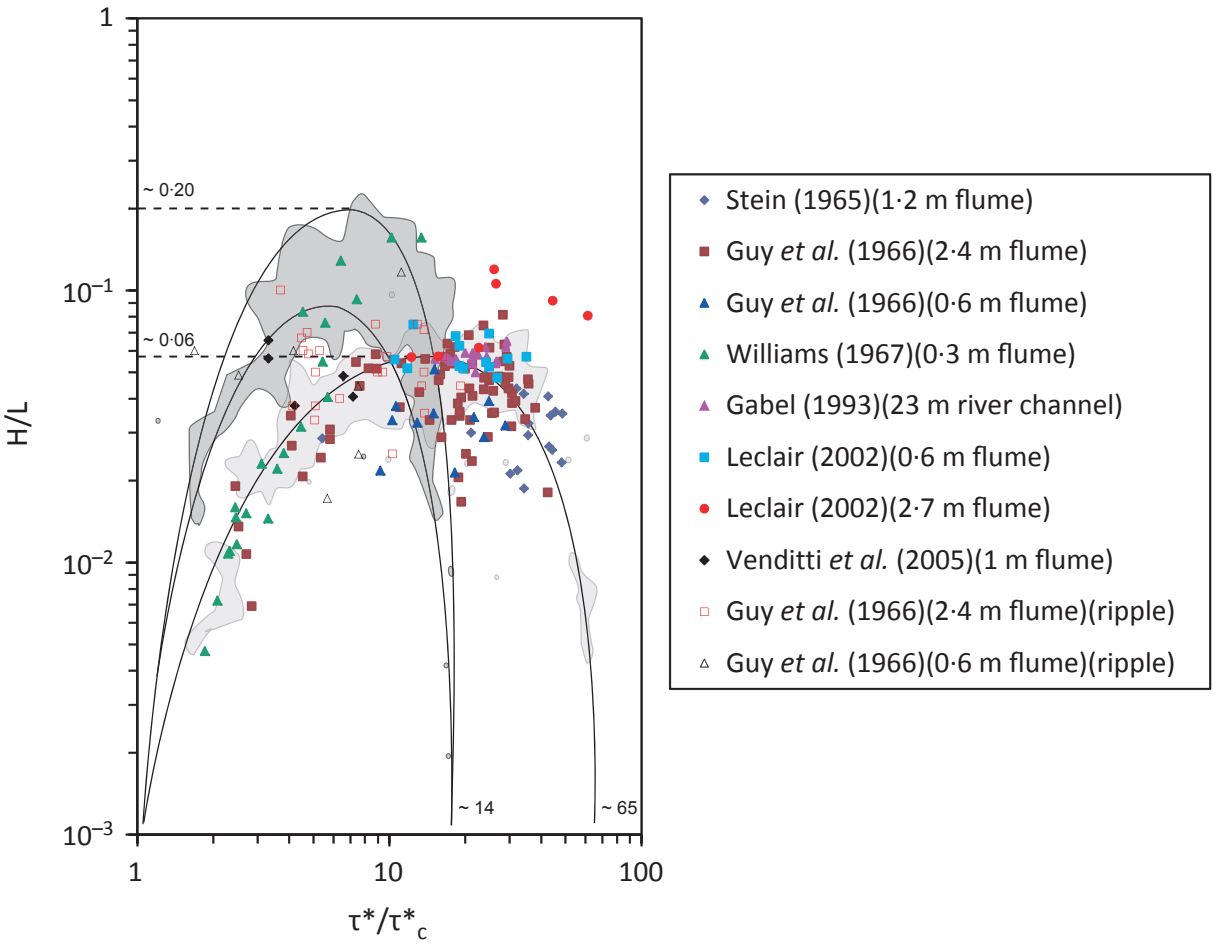

Fig. 1. The aspect ratio of equilibrium ripples and dunes plotted as a function of the transport stage, defined as the ratio of Shields number to the critical Shields number for sediment entrainment (τ_*/τ_{*c}), for all the data examined here. The dark and light shaded areas represent the data clouds for ripples and dunes, respectively (Venditti, 2013). The data clouds are drawn from the data compilation presented in Yalin (1972), as are the hyperbolas.

bedform normally decreases as its height increases to maintain constant sediment transport rate in a steady flow (Allen, 1973; Gabel, 1993; Coleman & Melville, 1994; Leclair, 2002; Bridge, 2003; Venditti *et al.*, 2005).

The influence of suspension on bedform dimensions and dynamics also supports the idea that transport stage influences bedform dynamics and migration rates. Observations show that high washload concentrations can influence dune morphology. Wan & Wang (1994) showed that, under a suspended load-dominated transport stage, the stability field of dunes was influenced by clay concentration, with dunes being replaced by upper stage plane beds at higher volumetric clay concentrations. Laboratory experiments also indicate that, at certain clay concentrations, the dune morphology may be significantly modified (Simons *et al.*, 1963; Wan, 1982). Others have documented changes from asymmetrical to symmetrical bedforms with lee slopes less than the angle of repose with greater suspended bed-material flux rates (Kostaschuk & Villard, 1996). Kostaschuk *et al.* (2009) show that this occurs because of deposition of suspended bed material in the dune trough. Collectively, these studies highlight the changes in bedform morphology that occur as suspended load increases, which must influence bedform migration rates.

Given the relations between transport stage and bedform geometry and the relation between bedform geometry and migration rates, it seems likely that there is a relation between bedform migration rate and transport stage that has remained relatively unexplored. Here, data available in the literature are used to explicitly define the relation between bedform migration rates and transport stage.

Table 1. Data sources used in the analysis.

Source	Data type	Channel width (*m*)	D_{50} (*mm*)	Observations that met criteria in methods	Observations used in analysis after outliers removed
Stein (1965)	Flume	1·22 (4 ft)	0·4	40	35
Guy *et al.* (1966)	Flume	2·43 (8 ft) 0·61 (2 ft)	0·19, 0·27, 0·28, 0·47, 0·93 0·32, 0·33, 0·54	116	113
Williams (1967)	Flume	0·30 (1 ft)	1·35	26	26
Gabel (1993)	Field	23	0·31–0·41	18	18
Leclair (2002)	Flume	0·6 2·7	0·43 0·81	20	20
Venditti *et al.* (2005)	Flume	1·0	0·5	5	4

METHODS

In order to explore the empirical relation between migration rate and transport stage, published data were selected where the following conditions were met: (i) bedform height, length and migration rate (V_b) were reported; (ii) information required to calculate the total shear stress and Shields number were reported; (iii) the flow was unidirectional; and (iv) bedform properties were measured when the original authors deemed the bedforms to be in 'equilibrium' with the flow. Equilibrium is reached when the mean properties of the bedform field cease to change with time. Data sets used in this study are listed in Table 1. Each observation is for the mean bedform properties measured at an imposed flow condition, rather than observations of individual bedforms. Bedform type (ripple or dune) was classified according to the original authors. The study by Guy *et al.* (1966) is the only data set that separates ripples and dunes. Unclassified bedforms were assumed to be dunes. Data from experiments by Guy *et al.* (1966) that were designed to examine the effects of temperature and high suspended sediment concentrations on bedform dimensions were excluded from the present study.

In order to calculate the transport stage, the Shields number (Eq. 1) was calculated using the shear stress calculated from the depth-slope product:

$$\tau = \rho_w g d S \qquad (2)$$

where d is flow depth and S is the water surface slope. The density of water was assumed to be 1000 kg m^{-3} and the density of sediment was assumed to be 2650 kg m^{-3}. Sidewall correc-

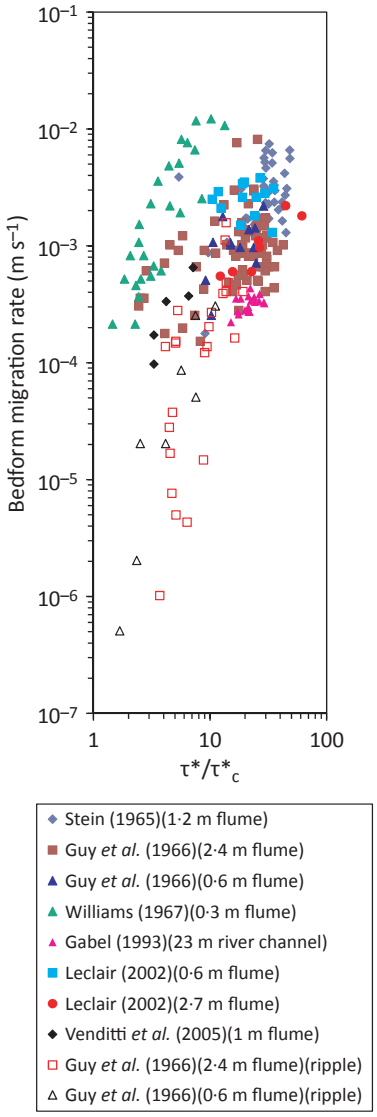

Fig. 2. Bedform migration rate versus transport stage (τ_*/τ_{*c}) for all the data listed in Table 1.

tions were implemented for flume data to calculate shear stress applied to the bed using the empirical equation of Williams (1970):

$$\tau_{\text{corrected}} = \frac{\tau}{(1 + 0 \cdot 18d/w^2)} \quad (3)$$

where w is the width of the flume. This shear stress represents the total shear stress applied to the bed including form and skin drag. Drag is not partitioned because a wide range of transport stages are examined, over which the bedform geometry changes significantly. Relations for partitioning drag over bedforms are not well-defined over this range of transport stages for field and laboratory conditions.

The goal was to define the *simplest possible relation* between the transport stage and bedform migration rates. To simplify the model, τ_{*c} was held constant at 0·03 through most of the calculations, except where specifically indicated. This approach is reasonable because the variation in the Shields curve is not substantial in the sand-sized range and it flattens for larger particles (Brownlie, 1981). This assumption may not be reasonable for fine sand, so the validity of the constant τ_{*c} assumption was assessed by calculating the critical Shields number, using the Brownlie (1981) fit to the Vanoni-Shields curve, and allowing it to vary in the model calculations where indicated.

RESULTS

Data assessment

The first step in the analysis was an examination of the observations to identify any eccentric data. The aspect ratio of bedforms was plotted as a function of τ_*/τ_{*c} in Fig. 1 and the bedform migration rate was plotted as a function of τ_*/τ_{*c} in Fig. 2. Several data points clearly do not fit the general patterns observed. The data from Williams (1967) are for bedforms developed in very coarse (D_{50} = 1·35 mm) sand and with a much narrower (0·305 m) flume than the rest of the data set. The data have high migration rates for a given τ_*/τ_{*c} compared with data from other sources (Fig. 2). These data were excluded in the analysis except when the data set is stratified by the depth to grain-size ratio and the Williams (1967) data form their own category, as well as

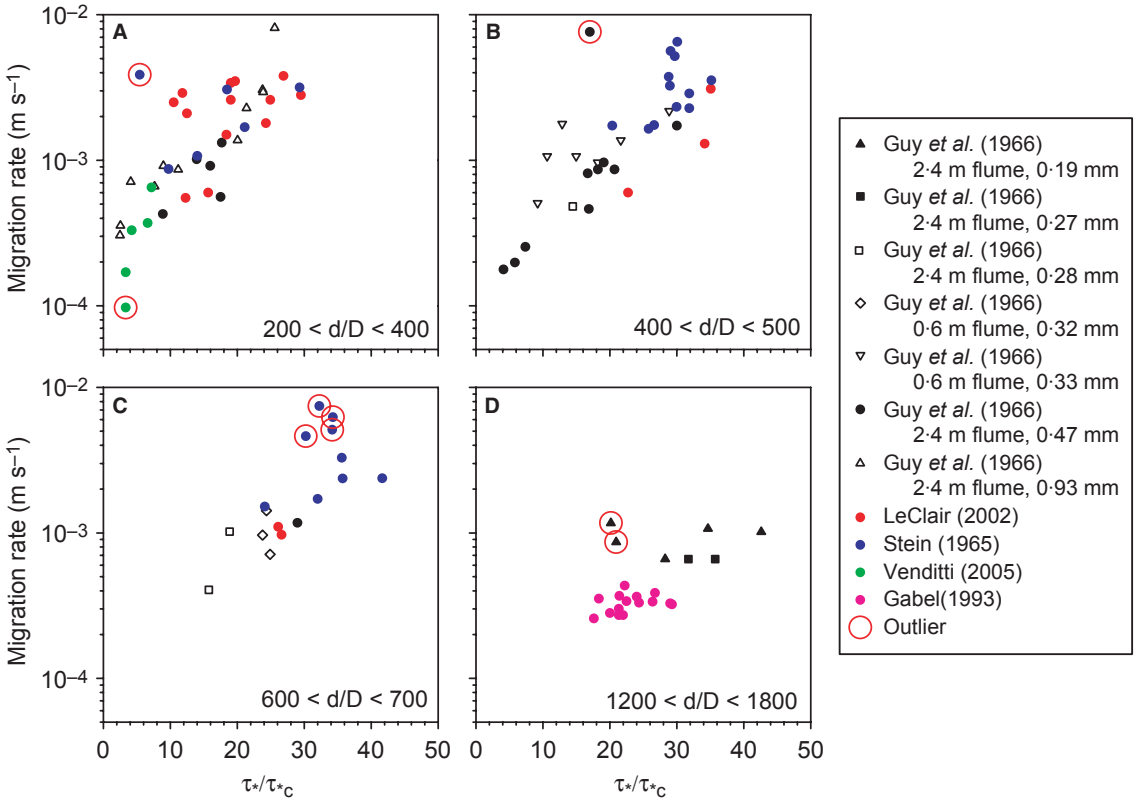

Fig. 3. Outliers identified in the data set for various ranges of the depth to grain-size ratio d/D: (A) 200 < d/D <400; (B) 400 < d/D <500; (C) 600 < d/D <700; and (D) 1200 < d/D <1800.

contributing to an adjacent category. Figure 3 shows that a number of other data points were also anomalous. They did not follow trends present within these experiments, meaning that high or low migration rates were found for a given grain size and shear stress. These included: (i) Runs 25, 26, 31, 32 and 35 from Stein (1965); (ii) Runs 8 and 32 from experiments in the 2·4 m (8 ft) wide flume and D_{50} = 0·19 mm from Guy *et al.* (1966); (iii) Run 75 from an experiment in the same flume with D_{50} = 0·47 mm from Guy *et al.* (1966); and (iv) Run E from Venditti *et al.* (2005). The specific reason why these runs had anomalous migration rates is not clear.

Bedform geometry and its relation to the Shields number

The aspect ratio of ripples and dunes included in the analysis is plotted as a function of transport stage in Fig. 2. The transport stage for ripple data ranges between 1·69 and 19·2 and ripple aspect ratio ranges between 0·0172 and 0·117. Data for dunes have a wider range of transport stages (2·45 to 61·5) and are generally lower amplitude (H/L ranges from 0·00690 to 0·119). The difference in the transport stage data range highlights the fact that ripples wash out to a flat bed at much lower shear stresses than dunes. The dune data used here clearly overlap the data cloud from Yalin (1972) and the broad pattern of increasing then decreasing aspect ratio with increasing transport stage is well-represented. The overlap between the ripple data and the Yalin (1972) data cloud is not obvious, but the data plotted here for ripples are very limited. The data of Williams (1967) have the steepest aspect ratios for a given grain size. Data from Leclair (2002) also appear to have anomalous aspect ratios (Fig. 1); however, the migration rates are entirely consistent with the rest of the data set. These experiments used the largest grain sizes in the data set [Williams (1967): 1·35 mm and Leclair (2002) 0·81 mm], suggesting that grain size plays a role in dune aspect ratio.

Regression analysis of all dune and ripple data

Ripple and dune and migration rate are plotted as a function of transport stage in Fig. 4A and B, respectively. The ripple data have a wider range of migration rates ($5{\cdot}08 \times 10^{-7}$ to $1{\cdot}58 \times 10^{-3}$ m sec^{-1}) than the dune data ($1{\cdot}52 \times 10^{-4}$ to $8{\cdot}13 \times 10^{-3}$ m sec^{-1}). Both ripple

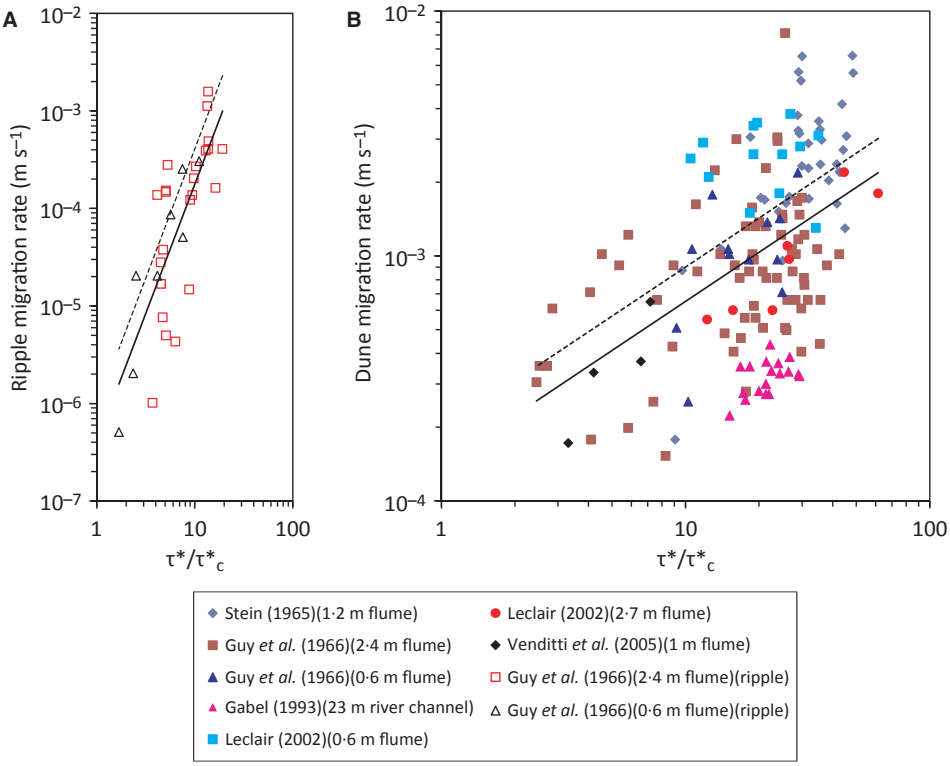

Fig. 4. Migration rate of (A) ripples and (B) dunes plotted against transport stage (τ_*/τ_{*c}) for the edited data set. Solid black lines are linear regressions (Table 2). Dashed black lines are regressions corrected using the BCF (bias correction factor).

Table 2. Summary of a, m, R^2 and P-value for ripple and dune data shown in Fig. 4.

Bedform type	n	Regression analysis intercept (a)	Regression analysis slope (m)	BCF	R^2	P-value
Dune	159	$1{\cdot}41 \times 10^{-4}$	0·666	1·35	0·232	$1{\cdot}25 \times 10^{-10}$
Ripple	31	$3{\cdot}96 \times 10^{-7}$	2·650	2·30	0·613	$1{\cdot}96 \times 10^{-7}$

and dune migration data show strong positive correlations, but the slopes of the relations vary considerably between ripples and dunes and amongst different dune data sets (Fig. 4B). Regression analysis of the ripple and dune data yields a power relation that has the form:

$$V_b = a\left(\frac{\tau_*}{\tau_{*c}}\right)^m \times \mathrm{BCF} \qquad (6)$$

where V_b is the bedform migration rate, a is the intercept, m is the slope and BCF is a bias correction factor. A bias arises when a log-transformed variable is retransformed back into its original units. A variety of methods have been proposed to correct the transform bias, but are all based on some estimate of the error in the regression and are nearly identical (Duan, 1983; Miller, 1984; Ferguson, 1986). The bias correction factor of Miller (1984) is used here:

$$\mathrm{BCF} = e^{\sigma^2/2} \qquad (7)$$

where σ is the standard error of the regression. The BCF is kept separate from a so its effect on the relation is clear. The values of a, m, BCF, the coefficient of determination (R^2) and the P-value are summarized in Table 2.

The relation between ripple migration rates and τ_*/τ_{*c} is statistically significant at the 99% confidence interval. The 99% confidence level is used to minimize the chance of accepting a non-significant result. The proportion of the variance in V_b explained by τ_*/τ_{*c} is 61% (Table 2). The relation between dune migration rate and transport stage is also statistically significant at the 99% confidence level, but <25% of the variation in V_b is explained by τ_*/τ_{*c}. In order to improve the explanatory power of the dune relation, the data set is stratified by two measures of relative roughness: H/d and d/D. The ratio of the bedform height to flow depth was explored with the expectation that height is a function of transport stage and therefore may influence the relation. The grain-size to flow depth ratio is explored with the understanding that grain size controls whether sediment will be suspended by a given flow. Yalin & Karahan (1979a) demonstrated that stratification by the inverse (D/d) improved the predictive power of parabolas fit through plots of aspect ratio and transport stage. Results are reported here using d/D because it produces integer category boundaries.

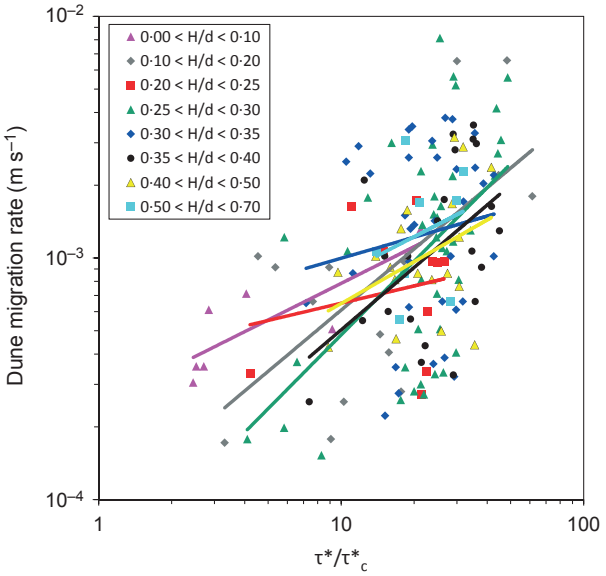

Fig. 5. Dune migration rate stratified by H/d. No BCF (bias correction factor) is applied to the lines.

Regression analysis for dune data stratified by the height to depth ratio (H/d)

Figure 5 shows the dune migration data stratified by H/d. Category boundaries were selected that were easy to distinguish and divided the data into groups with similar numbers of points. Small H/d represents low-amplitude bedforms compared to d; large H/d represent high-amplitude bedforms compared to d. It is clear from Fig. 5 that stratification by H/d does not reveal any underlying pattern in the relation between dune form and dune migration rate. Only one category ($0{\cdot}25 < H/d < 0{\cdot}3$) has a statistically significant relation at the 99% confidence interval. This category has the greatest number of data points (see Lin, 2011, for further details).

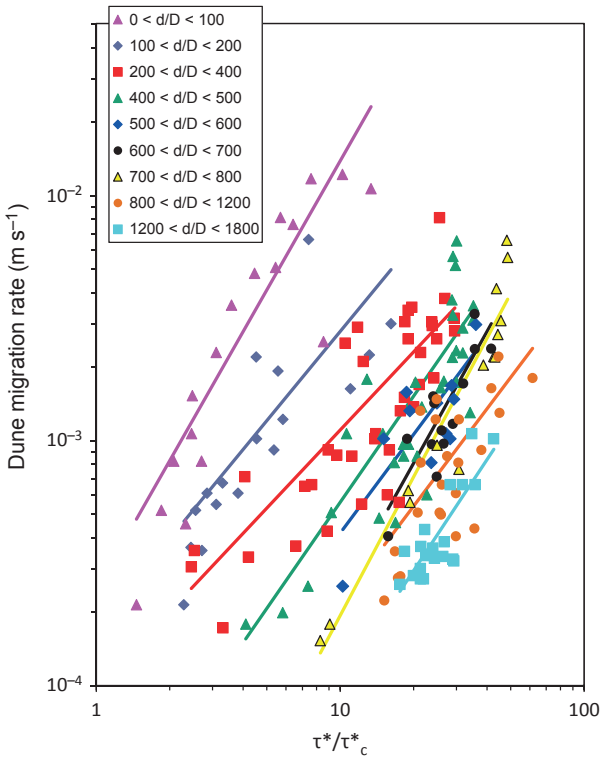

Fig. 6. Dune migration rate stratified by d/D. The BCF (bias correction factor) has been applied to all lines. See Table 3 for statistics.

Regression analysis for dune data stratified by the depth to grain-size ratio (d/D)

Figure 6 shows dune migration data stratified by d/D. Small d/D represents large grain size relative to flow depth and vice versa. Stratification by d/D produces a series of nearly parallel relations across the plot that all show that bedform migration rate increases with transport stage. The data of Williams (1967) have been included in Fig. 6 because they form their own category ($0 < d/D < 100$), as well as contributing to the $100 < d/D < 200$ category. The apparent eccentricity of the Williams (1967) data set seems to arise because the coarsest sediment bedforms have the highest migration rates. This suggests that the data are, in fact, not anomalous.

Each category in Fig. 6 yields a least-squares linear regression that has the same form as Eq. 6. The values of a, m, R^2, BCF, P-value and the standard error of the slope for each category are summarized in Table 3. All the relations between V_b and τ_*/τ_{*c} are statistically significant at the 99% confidence interval. The slope of the relations vary between 1·06 and 1·88, with a mean value of 1·48 (Table 3). Statistically, the slopes are not different in that the confidence intervals, calculated at the 99% confidence interval all overlap. The proportion of variation in V_b that is explained by τ_*/τ_{*c} averages 70% – much greater than for the unstratified data and the ripple data. The form of the relation is encouraging because the exponent is nearly equivalent to the 1·5 scaling often observed between shear stress and bedload transport rates (e.g. Meyer-Peter & Müller, 1948; Fernandez Luque & van Beek, 1976; Engelund & Fredsoe, 1976).

Regression intercepts and slopes

In order to assess the effect of holding τ_{*c} constant at 0·03, the regression slopes and intercepts from Table 3 were plotted in Fig. 7. There does not appear to be any trend in slope or R^2 across the d/D groupings. However, the intercept for $\tau_{*c} = 0{\cdot}03$ declines with increasing d/D, meaning that as grain size gets smaller relative to flow depth, the intercept declines. The dependence of the inter-

Table 3. Summary of a, m, and R^2 for each stratified d/D category plotted in Fig. 6 (assuming a constant critical Shields stress for sediment entrainment of 0·03).

Category (d/D)	n	Regression analysis intercept (a)	Regression analysis slope (m)	BCF	R^2	P-value	Standard error of slope
$0 < d/D < 100$	17	$2{\cdot}10 \times 10^{-4}$	1·75	1·17	0·813	$7{\cdot}55 \times 10^{-7}$	0·216
$100 < d/D < 200$	17	$1{\cdot}50 \times 10^{-4}$	1·21	1·15	0·676	$5{\cdot}17 \times 10^{-5}$	0·217
$200 < d/D < 400$	38	$8{\cdot}37 \times 10^{-5}$	1·06	1·15	0·657	$7{\cdot}04 \times 10^{-10}$	0·128
$400 < d/D < 500$	32	$1{\cdot}79 \times 10^{-5}$	1·44	1·14	0·715	$1{\cdot}13 \times 10^{-9}$	0·167
$500 < d/D < 600$	11	$1{\cdot}77 \times 10^{-5}$	1·34	1·08	0·624	$3{\cdot}83 \times 10^{-3}$	0·347
$600 < d/D < 700$	13	$3{\cdot}62 \times 10^{-6}$	1·79	1·05	0·733	$1{\cdot}87 \times 10^{-4}$	0·325
$700 < d/D < 800$	14	$2{\cdot}40 \times 10^{-6}$	1·88	1·06	0·923	$4{\cdot}72 \times 10^{-8}$	0·157
$800 < d/D < 1200$	23	$9{\cdot}28 \times 10^{-6}$	1·32	1·12	0·510	$1{\cdot}30 \times 10^{-4}$	0·282
$1200 < d/D < 1800$	20	$3{\cdot}09 \times 10^{-6}$	1·51	1·03	0·672	$9{\cdot}64 \times 10^{-6}$	0·249
Mean	21	$5{\cdot}53 \times 10^{-5}$	1·48	1·10	0·703	$4{\cdot}68 \times 10^{-4}$	0·232

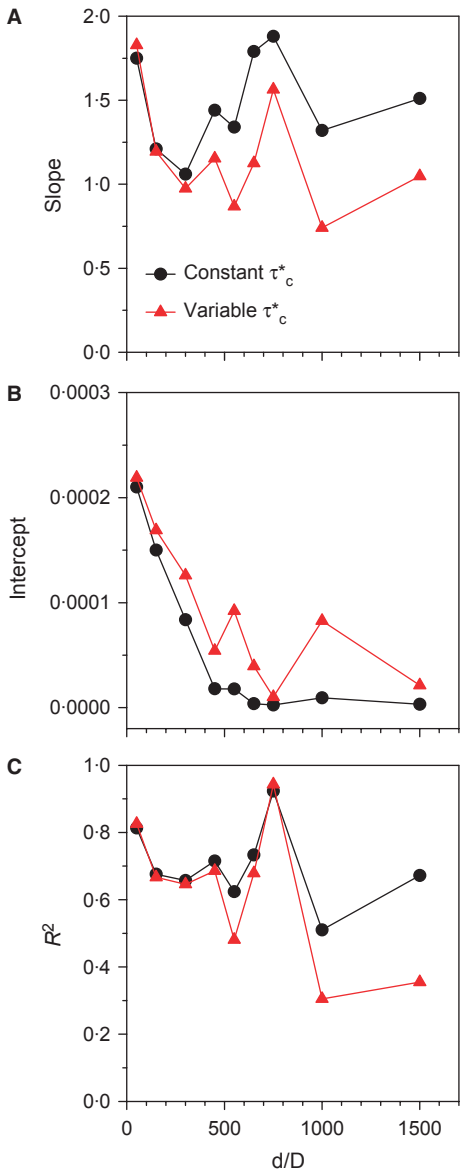

Fig. 7. Variation in (A) slope, (B) intercept and (C) R^2 using constant and variable critical Shields number for entrainment. All values were generated from regression analysis and are reported in Tables 3 and 4.

cept on d/D suggests that a threshold exists. This was explored here by allowing τ_{*c} to vary, calculating it for each observation using the Brownlie (1981) fit to the Shields diagram:

$$\tau_{*c} = 0.22\mathrm{Re}_*^{-0.6} + 0.06 \times 10^{-7.7\mathrm{Re}^{*-0.6}} \quad (8)$$

Re_* is the grain Reynolds number calculated as:

$$\mathrm{Re}* = \frac{u_* D}{\nu} \quad (9)$$

where $u* \equiv \sqrt{\tau/\rho_w}$ is the shear velocity and ν is the kinematic viscosity. A new set of slopes, intercepts and R^2 values were generated from regression analysis and plotted in Fig. 7 and reported in Table 4. These values are similar to those using a constant τ_{*c} in the calculation, but in finer sediment, relative to flow depth, the slopes of the relations are lower. This observation suggests that assuming $\tau_{*c} = 0{\cdot}03$ is a reasonable assumption for the coarser grain sizes relative to flow depth, but not for the finer grain sizes.

DISCUSSION

Bedform migration and its relation to sediment grain size

Dune and ripple migration rates show statistically significant positive correlations with transport stage. Ripple migration rate shows a higher correlation with τ_*/τ_{*c} than dunes, even though a weaker relation is expected for ripples because the data are from a much smaller pool ($n = 31$) than dunes ($n = 159$ without the outliers). The weaker relation for dunes reflects the greater scatter in the dune data set. Stratification of the dune data set by two measures of relative roughness (H/d and d/D) shows that dune migration rate is not influenced by dune geometry but is influenced by grain size.

It makes sense that mean bedform migration rates observed for a particular transport stage are not influenced by bedform geometry. It has been shown that individual bedform migration rate normally decreases as bedform height increases to maintain a constant sediment transport rate (Allen, 1973; Gabel, 1993; Coleman & Melville, 1994; Leclair, 2002; Venditti *et al.*, 2005). Such a relation between bedform height and migration rate is true for individual bedforms in a bedform field under the same flow because it takes longer to move a larger volume of sediment (larger bedform) than a smaller volume of sediment (small bedform) and maintain a constant sediment flux. Bedforms also propagate more slowly with an increase in height when they are developing from a flat bed (Coleman & Melville, 1994; Venditti *et al.*, 2005). Small bedforms that grow on the back of larger bedforms move faster than their host to accommodate the flux (Venditti *et al.*, 2005). This is because the group of bedforms moves as a whole package of sediment, so each part of the system has to move in proportion to its size. However, the migration data presented here are for fields of bedforms at equilibrium conditions and span a range of

Table 4. Summary of a, m, and R^2 for each stratified d/D category using a variable critical Shields stress for sediment entrainment.

Category (d/D)	n	Regression analysis intercept (a)	Regression analysis slope (m)	BCF	R^2	P-value	Standard error of slope
$0 < d/D < 100$	17	$2{\cdot}19 \times 10^{-4}$	1·83	1·16	0·826	$4{\cdot}50 \times 10^{-7}$	0·217
$100 < d/D < 200$	17	$1{\cdot}69 \times 10^{-4}$	1·20	1·15	0·667	$6{\cdot}30 \times 10^{-5}$	0·218
$200 < d/D < 400$	38	$1{\cdot}26 \times 10^{-4}$	0·98	1·15	0·646	$1{\cdot}20 \times 10^{-9}$	0·120
$400 < d/D < 500$	32	$5{\cdot}43 \times 10^{-5}$	1·15	1·15	0·686	$4{\cdot}90 \times 10^{-9}$	0·143
$500 < d/D < 600$	11	$9{\cdot}22 \times 10^{-5}$	0·87	1·11	0·481	$1{\cdot}80 \times 10^{-2}$	0·300
$600 < d/D < 700$	13	$3{\cdot}96 \times 10^{-5}$	1·13	1·06	0·679	$5{\cdot}40 \times 10^{-4}$	0·234
$700 < d/D < 800$	14	$1{\cdot}01 \times 10^{-5}$	1·56	1·04	0·943	$8{\cdot}00 \times 10^{-9}$	0·111
$800 < d/D < 1200$	23	$8{\cdot}28 \times 10^{-5}$	0·74	1·17	0·305	$6{\cdot}30 \times 10^{-3}$	0·244
$1200 < d/D < 1800$	20	$2{\cdot}13 \times 10^{-5}$	1·05	1·06	0·355	$5{\cdot}60 \times 10^{-3}$	0·333
Mean	21	$9{\cdot}04 \times 10^{-5}$	1·17	1·12	0·621	$3{\cdot}39 \times 10^{-3}$	0·213

transport stages, so the bedform size has little explanatory power in the derived relation.

The results indicate that bedforms formed in coarser sediments move faster than bedforms in finer sediments at the same transport stage. The specific reasons why finer sediment bedforms move more slowly is not clear from the data set. In a bed composed of larger sand grains, the particles would be expected to move more slowly than in a bed composed of finer grains at the same shear stress because of the increased mass of the coarser grains. This should make coarser bedforms slower than finer bedforms because the rate of bedload movement is proportional to particle velocity. Coarse sediment bedforms may move faster because the larger grains protrude higher into the flow and experience a greater drag force than smaller particles. Venditti *et al.* (2010) showed that coarser gravel particles can be transported faster than finer grains for this reason. However, this effect is likely to be more pronounced in mixed-size gravel because of differential protrusion of the grains. Sand tends to be more uniform in size, particularly in the experimental settings that dominate the data set, limiting differential protrusion.

Another potential reason that dunes in finer sediment move more slowly than in coarser sediment is suspension potential. McElroy & Mohrig (2009) argued that the bedform-related bed-material flux is composed of downstream translation (migration) and bedform deformation. Deformation is the change in the bedform shape. These authors argue that deformation must be equivalent to that proportion of the bed material that moves into temporary suspension over a dune. This is entirely consistent with the observation of Kostaschuk *et al.* (2009) who found that a significant portion of the suspended bed-material load is exchanged with the bed over a bedform. The amount of bedform deformation that occurs in a channel is certainly mitigated by grain size, whereby finer grains are more likely to be suspended than coarser grains at the same shear stress or transport stage.

The total bed-material flux in a sand-bedded channel with bedforms can be calculated from:

$$q_{sT} = \frac{A}{HL}(1-P)V_b H + q_{ss} \tag{10}$$

where A is the along stream cross-sectional area of the bedform, P is the porosity and q_{ss} is the suspended bed-material flux (Simons *et al.*, 1965; Venditti *et al.*, 2005). The term $A/(HL)$ is a bedform shape factor that has been reported to range from 0·5 to 0·6 for both laboratory-scale and field-scale dunes with a value of 0·55 often selected for calculations (Van den Berg, 1987; Ten Brinke *et al.*, 1999; Villard & Church, 2003; Venditti *et al.*, 2005). Consider two channels, one with a bed composed of fine sediment and another composed of coarse sediment, that both have the same sediment flux for a given transport stage. In the finer-grained channel, bedforms would either have to have a smaller bedform shape factor, be smaller in size or move more slowly to maintain the sediment flux because more sediment is moving in suspension. There is no evidence in the literature that bedform shape factors or size are controlled by grain size (Venditti, 2013), so slower moving bedforms in finer sediment is the logical response. The critical assumption here is that sediment flux rates are the same for a given transport stage, which is entirely consistent with a wide range of bedload transport equations (e.g. Meyer-Peter & Müller, 1948; Fernandez Luque & van Beek,

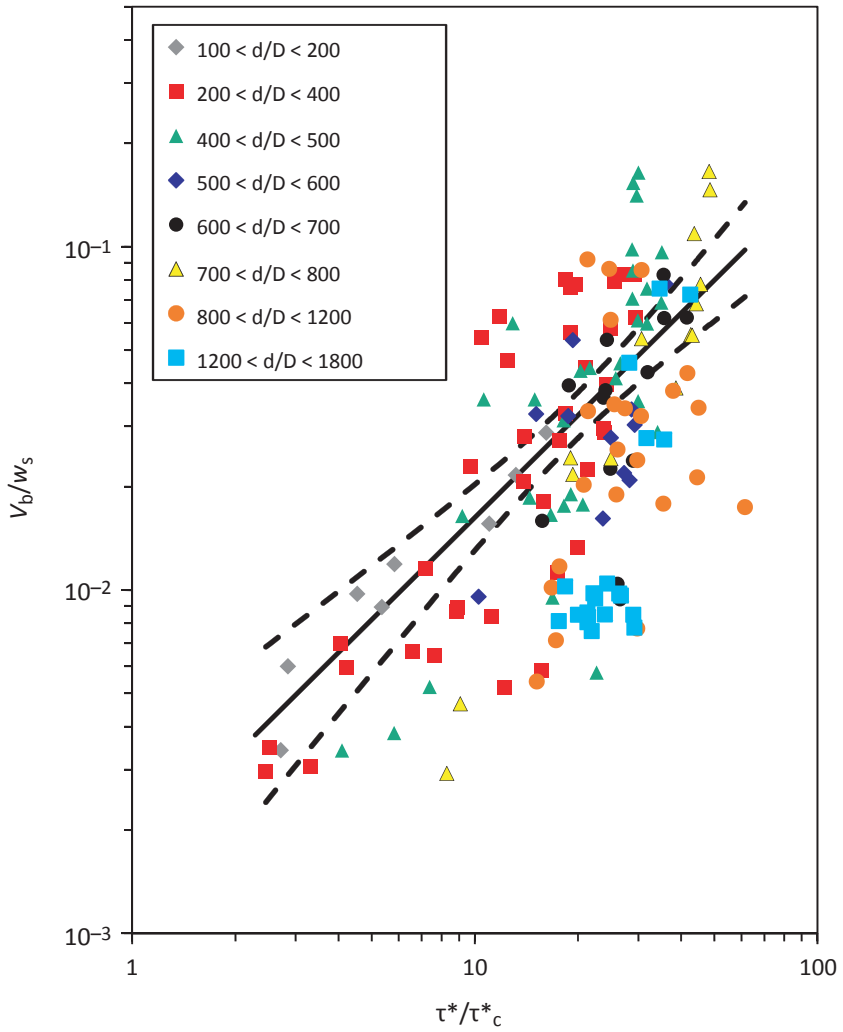

Fig. 8. Dimensionless migration rate (V_b/w_s) plotted against transport stage (τ_*/τ_{*c}) and stratified by d/D. The black line is the least-squared linear regression and the dashed lines are the 99% confidence intervals. The BCF (bias correction factor) has been applied.

1976; Engelund & Fredsoe, 1976), but is more difficult to justify when bed material is suspended. Nevertheless, bedforms are observed to move more slowly in finer sediments, where greater amounts of suspension occur at the same transport stage. Whether there is a causal link between suspension and bedform translation rate needs to be further explored.

Partial data collapse

The important role of suspension implied by the analysis suggests that the data may be collapsed onto a single curve if an appropriate scale can be found to make the bedform migration rate dimensionless. Figure 8 shows the dune migration made dimensionless by the grain fall velocity, w_s, calculated using the relations of Dietrich (1982). Bedform migration rate was also made dimensionless with the mean velocity and shear velocity, but that did not influence the paralleled groupings seen in Fig. 6. Least-squares regression analysis yields a relation in the following form:

$$\frac{V_b}{w_s} = 0.00127\left(\frac{\tau_*}{\tau_{*c}}\right)^{0.989} \times \mathrm{BCF} \qquad (11)$$

The BCF, calculated with Eq. 7, is 1·316. Dimensionless dune migration rate shows a positive correlation with τ_*/τ_{*c} with a slope near 1 (Fig. 8). The relation is statistically significant at the 99% confidence level ($P = 1{\cdot}73 \times 10^{-20}$) and 42% of the variation in V_b/w_s is explained by τ_*/τ_{*c}. While the amount of variability in V_b/w_s explained by τ_*/τ_{*c} is not great, the line appears well fit to the data. Nevertheless, the

degree of variability in the data and the apparent clustering of at least one grouping ($1200 < d/D < 1800$) below the line suggests that, for practical purposes, the d/D stratified relations (Fig. 6 and Table 3 for fixed τ_{*c} and Table 4 for variable τ_{*c}) are most appropriate for prediction.

Application in natural river channels

Application of models derived from laboratory data to natural channels should always be pursued with caution. The data sets examined here are all derived from laboratory channels, except one that comes from a small channel (Gabel, 1993). Data from large channels are absent in the analysis here because the information required to calculate various parameters is not available or because the flows are variable and are influenced by hysteresis effects (Allen, 1974, 1982) which would add scatter to the relations. This is particularly concerning because the pre-eminent bedforms in large channels tend to have a low lee angle morphology and are less asymmetrical than in smaller channels (Smith & McLean, 1977; Kostaschuk & Villard, 1996; Roden, 1998; Nittrouer *et al.*, 2008). Whether this dune morphology behaves differently in terms of migration rate is not known and needs to be examined.

The data required to test the models presented herein are difficult to find. Published observations of bedform migration rates in the field are remarkably scarce. Those available do not contain the observed water surface slopes required to estimate the total shear stress required as an input. However, rough estimates of the total shear stress suggest that the model can predict reasonable migration rates. Ilersich (1992) report bedform migration rates of $7{\cdot}85 \times 10^{-4}$ m sec^{-1} at low tide in the Fraser estuary where $D = 0{\cdot}3$ mm and the mean measured flow depth is 10·8 m. Water surface slopes were not measured during the measurements, but the water surface slope in Fraser estuary during flood flows is typically *ca* 5×10^{-5} (cf. Northwest Hydraulic Consultants, 2006). For these conditions, $\tau_* = 1{\cdot}1$, which is typical of single threaded sand-bedded river channels (Parker *et al.*, 2003; Parker, 2008). The transport stage, $\tau_*/\tau_{*c} = 36$ and Eq. 11 predict a migration rate of $18{\cdot}1 \times 10^{-4}$ m sec^{-1}, which is *ca* 2·3 times the observed migration rate. Given the level of variability in the data used to derive Eq. 11, the result is quite encouraging. Using Eq. 6, the coefficient values for variable critical shear stress and the largest d/D range in Table 4, the predicted migration rate is *ca* 1·2 times the observed rate, even though d/D is *ca* 36 000 for the Fraser River. Varying the high flow water surface slope in the estuary by ±50% gives V_b predictions between 0·6 and 1·9 times the observed rate, bounding the migration rate from Ilersich (1992). Although rough, these calculations suggest that the model does produce reasonable estimates of bedform migration, even for low angle dunes in large river channels and where bedforms are certainly adjusting to variable flow conditions.

A potential concern with the model presented is that it represents a very small range of suspended sediment concentrations. Natural river channels often have higher suspended sediment concentrations than laboratory flume channels and the material in suspension is washload that is much finer than the bed material. Dunes in flows with high suspended sediment concentrations have lower heights and migration rates relative to flow with low suspended sediment concentrations (Simons *et al.*, 1963; Wan, 1982). Simons *et al.* (1963) demonstrate that dunes show a distinguishable decrease in flow resistance, height and migration rate under flow with bentonite concentration greater than 5000 to 10 000 ppm ($1{\cdot}3 \times 10^4$ mg l^{-1} to $2{\cdot}7 \times 10^4$ mg l^{-1} assuming $\rho_s = 2650$ kg m^{-3}). Wan (1982) also shows that dune height decreases at bentonite concentrations greater than 7600 ppm ($2{\cdot}0 \times 10^4$ mg l^{-1}). In natural channels, sediment concentrations can vary widely, from negligible amounts up to $1{\cdot}5 \times 10^6$ mg l^{-1} in the Yellow River that drains the loess region of central China (Wan & Wang, 1994). The relations for estimating bedform migration rates might be expected to work reasonably well in rivers where suspended sediment concentrations are on the order of 10^2 mg l^{-1}. In rivers with suspended sediment concentrations approaching 10^4 mg l^{-1}, application of the relations should be approached cautiously.

CONCLUSIONS

The relation between bedform migration rates and transport stage, defined as the non-dimensional Shields stress divided by its value at the threshold for sediment entrainment, are examined using a field and several flume data sets. Both ripple and dune migration rates are positively correlated with transport stage. Ripple migration rates are better correlated with migration rates across a wide range of trans-

port stages. The relation between dune migration rates and transport stage is statistically significant, but less than 20% of the variability in migration rates is explained by transport stage because the role of grain size is not considered. Stratification of data by the ratio of the flow depth to grain size improved the amount of variability in migration rates that is explained by transport stage to *ca* 70%. This suggests that grain size exerts a strong control on bedform migration rates. As transport stage increases for a given depth to grain-size ratio, the migration rate increases. For a given transport stage, the migration rate increases as the depth to grain-size ratio gets smaller. It is not clear why this happens mechanistically from the available data, but it may be linked to the suspension threshold. Finer sediment is more easily suspended than coarser sediment at the same transport stage which may effectively slow bedforms in finer sediment. This assumes that the sediment flux rate is the same at a given transport stage, regardless of the grain size. Normalization of dune migration rates by the settling velocity of bed sediment partially collapses the data onto a single curve, which is remarkable given the wide range of data sources included in the analysis, differences in the way variables were measured and inherent experimental error within each data set. The empirical relations are primarily based on laboratory data. Application to a large channel with low lee angle dunes suggests that they do produce reasonable estimates of migration rate. Nevertheless, further explicit tests of the underlying relation in the laboratory and in the field are needed.

ACKNOWLEDGEMENTS

The authors contributed equally to this work. Funding for this research was provided by a NSERC Discovery Grant to JV. Early versions of this manuscript were kindly reviewed by Ted Hickin and Mike Church. The journal reviewers and editor provided valuable suggestions and input that greatly improved the manuscript.

REFERENCES

Allen, J.R.L. (1973) Features of cross-stratified units due to random and other changes in bed forms. *Sedimentology*, **20**, 189–202. doi:10.1111/j.1365-3091.1973.tb02044.x.

Allen, J.R.L. (1974) Reaction, relaxation and lag in natural sedimentary systems: general principles, examples and lessons. *Earth-Sci. Rev.*, **10**, 263–342.

Allen, J.R.L. (1982) *Sedimentary Structures: Their Character and Physical Basis*. Elsevier, New York, NY.

Bartholdy, J., **Ernstsen, V.B.**, **Flemming, B.W.**, **Winter, C.** and **Bartholomä, A.** (2010) A simple model of bedform migration. *Earth Surf. Proc. Land.*, **35**, 1211–1220. doi:10.1002/esp.2002.

Bridge, J.S. (2003) *Rivers and Floodplains: Forms, Processes, and Sedimentary Record*. Blackwell Science, Malden, MA, 504 pp.

Brownlie, W.R. (1981) *Prediction of Flow Depth and Sediment Discharge in Open Channels*. Report No. KH-R-43A. W. M. Keck Laboratory of Hydraulics and Water Resources, California Institute of Technology, Pasadena, CA, 232 pp.

Church, M. (2006) Bed material transport and the morphology of alluvial river channels. *Annu. Rev. Earth Planet. Sci.*, **34**, 325–354. doi:10.1146/annurev. earth.33.092203.122721.

Coleman, S. E. and **Melville, B. W.** (1994) Bed-form development. *J. Hydraul. Eng.*, **120**, 544–560.

Dade, W.B. and **Friend, P.F.** (1998) Grain-size, sediment transport regime, and channel slope in alluvial rivers. *J. Geol.*, **106**, 661–676. doi:10.1086/516052.

Dietrich, W.E. (1982) Settling velocity of natural particles. *Water Resour. Res.*, **18**, 1615–1626. doi:10.1029/WR018i006p01615.

Duan, N. (1983) Smearing estimate – a nonparametric retransformation method. *J. Am. Stat. Assoc.*, **78**, 605–610.

Engelund, F. and **Fredsoe, J.** (1976) A sediment transport model for straight alluvial channels. *Nord. Hydrol.*, **7**, 293–306.

Ferguson, R.I. (1986) River loads underestimated by rating curves. *Water Resour. Res.*, **22**, 74–76.

Fernandez Luque, R. and **van Beek, R.** (1976) Erosion and transport of bedload sediment. *J. Hydraul. Res.*, **14**, 127–144.

Gabel, S.L. (1993) Geometry and kinematics of dunes during steady and unsteady flows in the Calamus River, Nebraska, USA. *Sedimentology*, **40**, 237–269. doi:10.1111/j.1365-3091. 1993.tb01763.x.

Guy, H.P., **Simons, D.B.** and **Richardson, E.V.** (1966) Summary of alluvial channel data from flume experiments, 1956-61. *U.S. Geol. Surv. Prof. Pap.*, **462-I**, 1–96.

Ilersich, S.A. (1992) Bedforms and bedload treansport: evaluating rate equations in the Fraser River. MSc thesis, University of Guelph, British Columbia.

Kostaschuk, R.A. and **Villard, P.V.** (1996) Flow and sediment transport over large subaqueous dunes: Fraser River, Canada. *Sedimentology*, **43**, 849–863.

Kostaschuk, R., **Shugar, D.**, **Best, J.**, **Parsons, D.**, **Lane, S.**, **Hardy, R.** and **Orfeo, O.** (2009) Suspended sediment transport and deposition over a dune: Río Paraná, Argentina. *Earth Surf. Proc. Land.*, **34**, 1605–1611.

Leclair, S.F. (2002) Preservation of cross-strata due to the migration of subaqueous dunes: an experimental investigation. *Sedimentology*, **49**, 1157–1180. doi:10.1046/j.1365-3091. 2002.00482.x.

Lin, C.-Y. M. (2011) Bedform migration in rivers. M.Sc. Thesis, Simon Fraser University, Burnaby, British Columbia, Canada, 147 pp.

McElroy, B. and **Mohrig, D.** (2009) Nature of deformation of sandy bed forms. *J. Geophys. Res.*, **114**, F00A04. doi: 10.1029/2008JF001220.

Meyer-Peter, E. and **Müller, R.** (1948) Formulas for bed-load transport. *Proceedings, 2nd Congress, International Association of Hydraulic Research*, pp. 39–64. International Association of Hydraulic Research, Stockholm, Sweden.

Miller, D.M. (1984) Reducing transform bias in curve fitting. *Am. Stat.*, **34**, 124–126.

Miller, M.C., **McCave, I.N.** and **Komar, P.D.** (1977) Threshold of sediment motion under unidirectional currents. *Sedimentology*, **41**, 883–903.

Mohrig, D. and **Smith, J.D.** (1996) Predicting the migration rates of subaqueous dunes. *Water Resour. Res.*, **32**, 3207–3217.

Nittrouer, J.A., **Allison, M.A.** and **Campanella, R.** (2008) Bedform transport rates for the lowermost Mississippi River. *J. Geophys. Res.*, **113**, F03004. doi: 10.1029/2007JF000795.

Northwest Hydraulic Consultants (2006) Final Report: Lower Fraser River Hydraulic Model. Report to Fraser Basin Council, December, 2006.

Parker, G. (2008), Transport of gravel and sediment mixtures, In *Sedimentation Engineering, ASCE Man* (Ed M.H. Garcia), vol. **110**, pp. 165–252, Am. Soc. Civ. Eng., Reston, Va.

Parker, G., **Toro-Escobar, C.**, **Ramey, M.** and **Beck, S.** (2003) Effect of floodwater extraction on mountain stream morphology. *J. Hydraul. Eng.*, **129**, 885–895.

Raudkivi, A.J. (1967) *Loose Boundary Hydraulics*. Oxford, Pergamon.

van Rijn, L.C. (1984) Sediment transport III: bed forms and alluvial roughness. *J. Hydraul. Eng.*, **110**, 1733–1754.

Roden, J.E. (1998) The sedimentology and dynamics of mega-dunes, Jamuna River, Bangladesh. PhD thesis, School of Earth Sciences and School of Geography, University of Leeds, United Kingdom, 310 pp.

Simons, D.B., **Richardson, E.V.** and **Haushild, W.L.** (1963) Some effects of fine sediment on flow phenomena. *U.S. Geol. Surv. Prof. Pap.*, **1489-G**, 1–47.

Simons, D.B., **Richardson, E.V.** and **Nordin, C.F.** (1965) Bedload equation for ripples and dunes. *U.S. Geol. Surv. Prof. Pap.*, **462-H**, 1–9.

Smith, J.D. and **McLean, S.R.** (1977) Spatially-averaged flow over a wavy surface. *J. Geophys. Res.*, **82**, 1735–1746.

Stein, R.A. (1965) Laboratory studies of total load and apparent bed load. *J. Geophys. Res.*, **70**, 1831–1842. doi:10.1029/JZ070i008p01831.

Ten Brinke, W.B.M., **Wilbers, A.W.E.** and **Wesseling, C.** (1999) Dune growth, decay and migration rates during a large-magnitude flood at a sand and mixed-gravel bed in the Dutch Rhine river system. In: *Fluvial Sedimentology VI* (Eds. N.D. Smith and J. Rogers), *Spec. Publ. Int. Assoc. Sedimentol.*, **28**, 15–32, Blackwell Science, Malden, MA.

Van den Berg, J.H. (1987) Bedform migration and bed-load transport in some rivers and tidal environments. *Sedimentology*, **34**, 681–698. doi:10.1111/j.1365-3091.1987.tb00794.x.

Venditti, J.G. (2013) Bedforms in sand-bedded rivers, In: *Treatise on Geomorphology* (Eds. J. Shroder, Jr and E. Wohl), pp., *Fluvial Geomorphology, 9,* 137–162. Academic Press, San Diego, CA.

Venditti, J.G., **Church, M.** and **Bennett, S.J.** (2005) Morphodynamics of small-scale superimposed sand waves over migrating dune bed forms. *Water Resour. Res.*, **41**, W10423. doi:10.1029/2004WR003461.

Venditti, J.G., **Dietrich, W.E.**, **Nelson, P.A.**, **Wydzga, M.A.**, **Fadde, J.** and **Sklar, L.** (2010) Mobilization of coarse surface layers in gravel-bedded rivers by finer gravel bed load. *Water Resour. Res.*, **46**, W07506. doi:10.1029/2009WR008329.

Villard, P.V. and **Church, M.A.** (2003) Dunes and associated sand transport in a tidally influenced sand-bed channel: Fraser River, British Columbia. *Can. J. Earth Sci.*, **40**, 115–130. doi:10.1139/e02-102.

Wan, Z. (1982) Bed material movement in hyperconcentrated flow. Ser. Pap. 31, Inst. of Hydrodyn. and Hydraul. Eng., Tech. Univ. of Den., Lyngby, Denmark.

Wan, Z. and **Wang, Z.** (1994) *Hyperconcentrated Flow*. A. A. Balkema, Rotterdam, the Netherlands.

Williams, G. P. (1967) Flume experiments on the transport of a coarse sand. *U.S. Geol. Surv. Prof. Pap.*, **562-B**, 1–31.

Williams, G. P. (1970) Flume width and water depth effects in sediment-transport experiments. *U.S. Geol. Surv. Prof. Pap.*, **562-H**, 1–37.

Yalin, M.S. (1972) *Mechanics of Sediment Transport*. Pergamon Press, Oxford.

Yalin, M.S. and **Karahan, E.** (1979a) Steepness of sedimentary dunes. *J. Hydrol. Div.*, **105**, 381–392.

Yalin, M.S. and **Karahan, E.** (1979b) Inception of sediment transport. *J. Hydrol. Div.*, **105**, 1433–1443.

Manuscript received 21 August 2012; revision accepted 22 April 2013